International Journal of Future Generation Communication and Networking
Vol. 13, No. 2, (2020), pp. 554 – 566

Design of Quazi-Z-Source Inverter with SSE-RNN Controller for Grid-Connected Hybrid Renewable Energy Sources

Ratheesh. S
Director-Research and Development, Sea Sense Softwares Private Limited

Abstract

Due to the load variations and different impedance, the unbalanced voltages and harmonics usually occur. In this paper, we proposed a quasi-Z-source inverter (qZSI) with SSE-RNN controller for grid connected renewable energy sources (RES). The SSE-RNN is the combination of the salp swarm algorithm (SSA) with Elman-recurrent neural network (E-RNN). Here, hybrid RES such as PV and wind are used, and buck-boost converter is employed. To get exact power, SSE-RNN controller is used, which is the combination of the salp swarm algorithm and Elman-recurrent neural network for tuning the gate pulse of the inverter. E-RNN operation will be enhanced by SSA to make less harmonic controller voltage. When compared with other metaheuristic algorithms, the SSA gives better results using convergence rate and complexity issues. Thus we get the error-free output voltage without harmonic distortions. The performance outcome is inverter voltage and current, grid current, DC link voltage, grid voltage, and the analysis of THD, which is taken in the MATLAB/Simulink platform. The performance of THD and DC link voltage is compared with other existing techniques.

Keywords: *Renewable Energy Sources, Converter, Inverter, Salp Swarm Algorithm and Elman-Recurrent Neural Network.*

1. Introduction

Nowadays the electricity generations are coming from renewable energy sources like hydro, geothermal, photovoltaic (PV), biomass, tidal, wind, and so on. Till 2014, RES contributed 22.8% of global electricity in the world [1-2]. From PV, the amount of electricity it produced directly, which relies upon the sunlight. The wind has a positive network effect if the grid is connected to PV. During the latest year, the extension in the usage of RES has pulled in consideration of research community [3]. In many case, reliably and productively there is a combination with utility grid is remain a challenge. To defeat this new difficulty, one of the significant solutions is microgrid. The microgrid can utilize different components for controlling the grid power profile [4-5]. To an energy management system, an adequate method is linked to getting an efficient performance of microgrid.

The demand for RES has increased significantly due to the shortage of fossil fuels and greenhouse effects. The PV and wind are mostly used in day to day life for many applications [6]. The demand for PV over the past 20 years has grown consistently by 20% to 25%, which is mainly because of decreasing cost and prices [7]. PV inverter is used to convert dc power into ac power, which is obtained from PV molecules to be fed into the grid. The wind is created by the unequal heating of the Earth's surface by the sun. The availability of wind vigorously varies regarding time [8]. Thus, the wind energy output system won't have permanent frequency and voltage magnitude. By using an uncontrolled rectifier, the AC voltage can be transformed to DC voltage, which is generated by wind and then, be controlled using a converter [9]. The power conversion scheme can transmit the power from the cell to the load, which continuously needs high efficiency. Still, from the solar cell, the output power is easily changed by the environmental conditions like temperature and irradiation. Depending upon the load type, the switching conditions are dc-ac inverter or dc-dc converter [10].

To get the extreme power, the MPPT algorithm is used, which tracks the maximum power from PV and wind. From the PV panel, to convert the direct voltage or current, the different levels of inverters are utilized [11-13]. The conventional voltage source inverter suffers from higher switching losses, higher harmonics, higher voltage stress, the output voltage of AC cannot exceed the DC link voltage, and higher electromagnetic interferences. The harmonics are removed by using filters to get the clear output [14]. The power quality issues like swell, sag, seventh, and fifth-order harmonics are presented in the system; PD, PID may avoid this, and PI controllers, however, this controller may not be effective [15]. The above-mentioned problem can be solved by utilizing the control strategy. The novel control

ISSN: 2233-7857 IJFGCN

method is tuned to the gate pulse of the novel inverter with optimization algorithms. Thus we get the error free output voltages without any harmonic distortions.

A key contribution of the proposed system is given as follows,

- Design hybrid renewable energy sources (i.e., PV and wind model).
- Design of novel converter (i.e., Buck-Boost) to adjust the power level from the output.
- To design quasi-Z-source inverters to get the maximum power.
- Design the SSE-RNN controller to tune the gate pulse of the inverter.
- Thus we get error free harmonic less output voltages with less THD.

The rest of the paper is organized as follow, the next section gives the related works. Section three gives the detailed explanation about the hybrid RES with PV and wind, hybrid Buck-Boost converter, qZSI and SSE-RNN controller. The results and discussion is presented in next section. Final section gives the proposed conclusion.

2. Related Work

For residential applications, Jafari et al. [16] presented a magnetic coupled RES. By using multi-winding magnetic link, a battery, fuel cell stack and PV panels are integrated to supply a residential load, which can work in off-grid operation, and multi grid connected nodes. An energy management unit included Off-line dynamic programming based optimization step. According to provided energy plan, a real time rule based controller was calculated to control the power optimally. Hardware design, energy management techniques, control techniques, and steady-state oscillations are studied variously.

One of the dominant factor is energy storage. It can enhance system flexibility, reduce power fluctuations and dispatch of electricity which was generated by different RES like solar and wind. In PV and wind system, Rekioua et al [17] used the various storage. The various mathematical models are listed and mostly utilized batteries are summarized. It is the two technologies i.e. supercapacitor and batteries had various characteristics. In electric vehicle, the fuel cells and batteries are presented for various applications.

Chakir et al [18] presented a system of grid connected PV battery that may mange its flow of energy by optimal management algorithm. The connection of DC bus source tackles the synchronization problems among source and loads. Battery charging and discharging power gives an extension of battery life. According to their mathematical modelling, they simulated the dynamic behavior of various components architecture. To serve the load power, an energy management algorithm was implemented.

For wind power smoothing, Guo et al [19] presented a robust dynamic wavelet method by hybrid energy storage system (HESS) which consist of super capacitor and batteries. The state of charge of HESS for power injection regulation which allows charge and discharge depth. In an optimal manner, the supercapacitor and batteries can be coordinated which yields high efficiency. The wind power prediction was established to remove the uncertainty of wind power.

In PV and wind, the MPPT method is mostly utilized by Rekioua et al [20]. In optimization, the mostly utilized control methods acts on duty cycle automatically to place the generator at its optimal value. The algorithm consist of two types i.e. advanced and classical. Summarized the MPPT method which was utilized in PV and wind system. Based on partial shading conditions, the PV system of global maximum power point tracking method was given in the study.

This paper deals with grid perturbations like harmonic distortions, unbalance voltages, balanced voltage dips and unbalanced current. Due to the load variations and different impedance, the unbalanced voltage usually occur. Essentially, due to the system impedance and voltage unbalances, the current unbalance is caused. Due to short circuit the voltage dips are occur in power system. Faults and transformer energizing are the main causes which are present in the voltage dips and in the distribution system the harmonics are appeared. This can be overcome by the proposed method.

3. Proposed Methodology

Design and analysis of qZSI with SSE-RNN controller for grid connected hybrid renewable energy sources is presented in this paper. SSE-RNN controller is used to reduce the power fluctuation, THD, unbalanced voltages and unbalanced current in microgrid. Here, hybrid RES such as PV and wind is used and buck boost converter is used. To get exact power, SSE-RNN controller is used which is the combination of salp swarm algorithm and Elman-recurrent neural network for tuning the gate pulse of

ISSN: 2233-7857 IJFGCN

the inverter. This controller will compensate the load voltage and load current distortion and it also balances and unbalances load at single iterations. The proposed work flow is shown in figure 1.

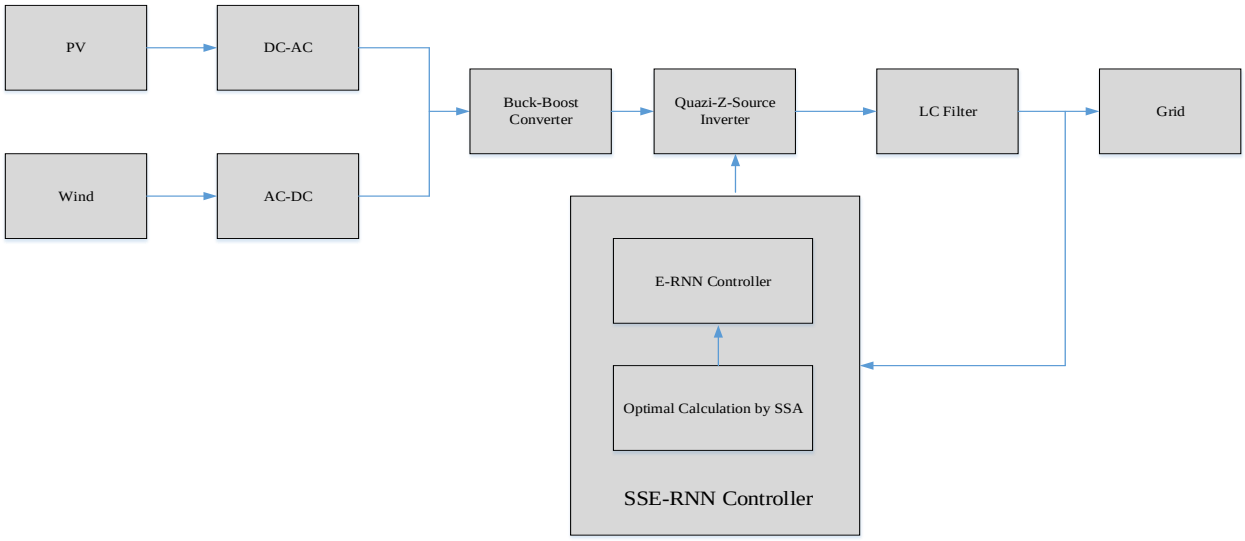

Figure 1. Proposed Work Flow

In proposed work, the performance of inverter totally relies on E-RNN controller which is tuned by SSA optimization algorithm. The E-RNN operation will be calculated by SSA to make less harmonic controller voltage. When compared with other metaheuristic algorithms, the SSA gives better results by means of convergence rate and complexity issues. So this is the main purpose for choosing SSA to optimize the E-RNN controller. By assuming various modulation indices the data required for SSE-RNN is obtained by solving harmonics equations. Here, at inverter side, LC filter is used to improve the output due to the generation of less harmonic output voltages. Thus proposed SSE-RNN perform better in THD and reduced the design complexity.

3.1. Mathematical Modelling of RES

The various electrical components combined to form hybrid RES. These components are PV, wind, inverter battery bank, controller and other devices. To assess the exhibition of hybrid system each components needs to be modelled separately. Figure 2 depicts hybrid RES such as PV and wind.

Figure 2. Hybrid PV-Wind

3.1.1. Mathematical Modelling of PV array: A solar PV array system is a joined components which reveals improvement of amount of PV cell in shunt and series. In an array the joined modules is similar as in module. One PV panel is used to make out the PV. To produce power from sun the additional hardware of electrical and mechanical are used.

ISSN: 2233-7857 IJFGCN

The expression for PV cell of I is given by,

$$I = I_{PH} - I_D - I_{RS} \tag{1}$$

Where, I is represented as PV cell, current of PV is denoted as I_{PH} , polarization of p-n junction current is represented as I_D and I_{RS} is denoted as resistor current.
The parameter will shifts as indicated during the temperature and isolation state by the below conditions.

$$\Delta\tilde{T}_{cl} = \tilde{T}_{cl} - \tilde{T}_{stc} \tag{2}$$

$$\Delta I = \alpha_{SC}\left(\frac{G}{G_{STC}}\right)\Delta\tilde{T}_{cl} + \left(\frac{G}{G_{STC}} - 1\right)I_{SC,STC} \tag{3}$$

Where, $\tilde{T}_{cl}$ is represented as cell temperature, level of irradiance is represented as G.
The voltage condition of PV cell is assumed based on normal situation by,

$$\Delta V = -\beta_{OC}\Delta\tilde{T}_{cl} - R_S\Delta I \tag{4}$$

Where, I is represented as PV cell, R_S is represented as resistance and ΔV is denoted as voltage source.

3.1.2. Mathematical Modelling of Wind Energy System: This section explain the mathematical modelling of wind power generation.

The coefficient of power is calculated as follow

$$C_P = \frac{2.P_{wind}}{\delta.R.V^3{}_{wind}} \tag{5}$$

Where, R is represented as rotor blades, $P\&V$ is represented as power and voltage.
The power and torque equation is calculated as follow

$$Power_{WIND} = \frac{1}{2}C_p(\delta).\rho.R.V^3{}_{wind} \tag{6}$$

$$Torque_{WIND} = t_{mec} = \frac{1}{2}\ \frac{C_p(\delta).\rho.r.R.v^2{}_{wind}}{\delta} \tag{7}$$

Where, the coefficient of power is denoted as C_P , ratio of tip speed is represented as δ density of air is represented as ρ , rotor radius is represented as r .

3.2. Buck Boost Converter

DC to DC converter is generated in buck boost converter. The DC to DC converter output voltage is smaller than or higher than input voltage. The magnitude output voltage is based on duty cycle. The other name of Buck boost converter is step down and step up transformer. The input and output power is equal by using the low conversion energy. Figure 3 shows the equivalent buck boost circuit.

ISSN: 2233-7857 IJFGCN

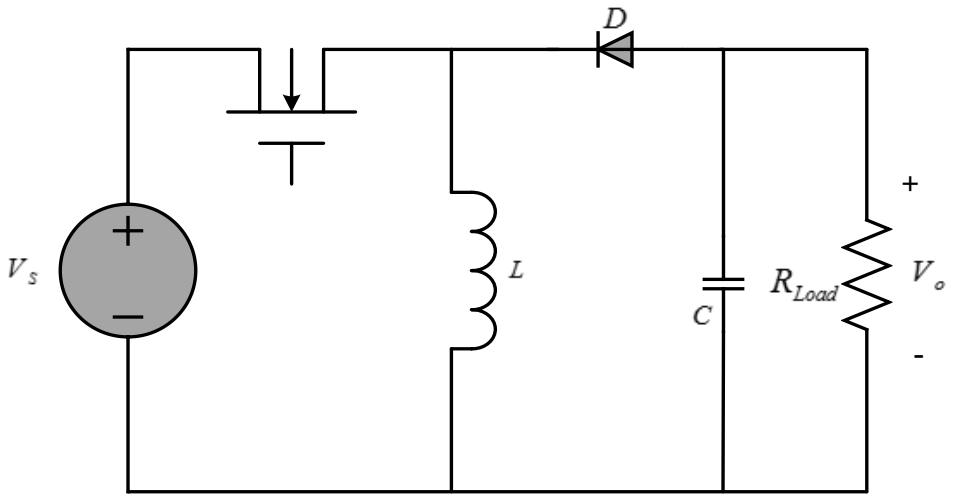

Figure 3. Equivalent Buck Boost Converter Circuit

If the switching device is ON, the voltage from input is applied through the inductor. Same time, the load from capacitor C is partially discharged and the inductor current linearly increases. The inductor voltage reverses in polarity and the diode is forward biased if the switching device is OFF.
The output voltage of steady state can be gotten from the equation (8)

$$\frac{V_0}{V_g} = -\frac{D}{1-D} \tag{8}$$

Where, output voltage is denoted as V_0, duty cycle is represented as D.
The expression of current is as follow

$$\frac{I_o}{I_{in}} = -\frac{1-D}{D} \tag{9}$$

Where, input current is denoted as I_{in} and output current is given as I_o.
Therefore from these two expression,

$$R_{in} = \frac{V_{in}}{I_{in}} = \frac{D^2}{(1-D)^2} \times \frac{V_o}{I_o} \tag{10}$$

$$R_{in} = \frac{V_{in}}{I_{in}} = \frac{D^2}{(1-D)^2} \times R_{Load} \tag{11}$$

Where, resistive load is represented as R_{Load} and duty cycle varies from 0 to 1, thus an output voltage is generated by a buck boost converter.

3.3. Quasi-Z-source Inverter

The equivalent circuit of qZSI is shown in figure 4. At DC side, qZSI has two modes such as shoot through state (STS) and non-shoot through state (NSTS) (i.e. conventional zero state and active state). The diode and unique LC filter are joined to the inverter bridge which change the circuit procedure.

ISSN: 2233-7857 IJFGCN

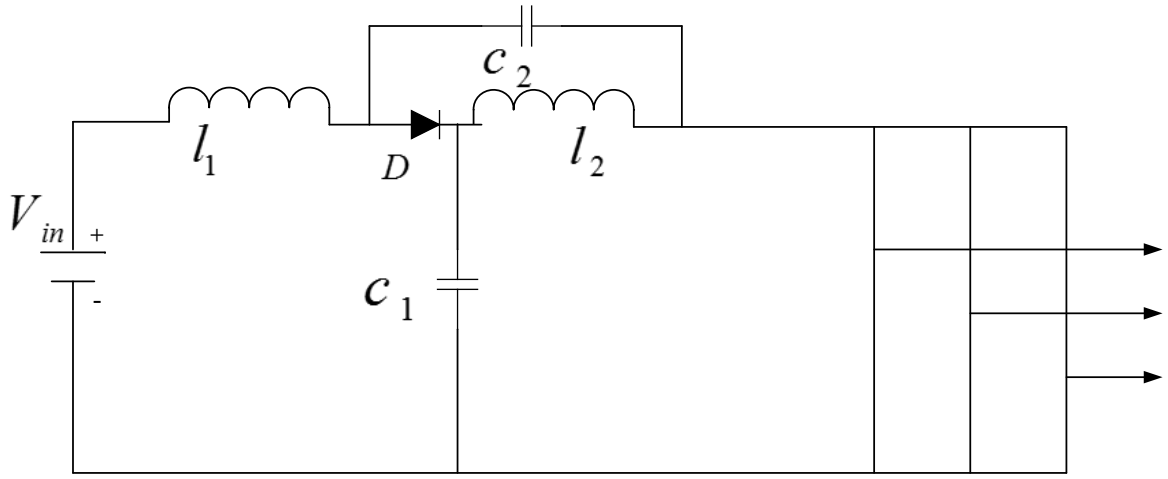

Figure 4. Equivalent Circuit of qZSI

3.3.1. NSTS: The inverter bridge is equivalent to the current sources in the NSTS. Let us assume, one switching cycle interval is $\tilde{T}$, STS interval is represented as $\tilde{T}_o$, NSTS is represented as $\tilde{T}_1$ thus,

$$\tilde{T} = \tilde{T}_0 + \tilde{T}_1 \tag{12}$$

Duty ratio of STS is as bellow,

$$D = \frac{\tilde{T}_o}{\tilde{T}_1} \tag{13}$$

The NSTS corresponding equation is given as follow,

$$\bar{V}_{l1} = \bar{V}_{in} - \bar{V}_{c1} \tag{14}$$

$$\bar{V}_{l2} = -\bar{V}_{c2} \tag{15}$$

$$\bar{V}_{PN} = \bar{V}_{c1} - \bar{V}_{l2} = \bar{V}_{c1} + \bar{V}_{c2} \tag{16}$$

$$\bar{V}_{diode} = 0 \tag{17}$$

Where, $\bar{V}_{l1}$ and $\bar{V}_{l2}$ are the inductor voltages; $\bar{V}_{c1}$ and $\bar{V}_{c2}$ are the capacitor voltages of the impedance network.

3.3.2. STS: In the traditional voltage source inverter (VSI) this state is forbidden, because it will cause voltage source short circuit and harm the devices.
The shoot through state corresponding equation is given as follow,

$$\bar{V}_{l1} = \bar{V}_{in} + \bar{V}_{c2} \tag{18}$$

$$\bar{V}_{l2} = \bar{V}_{c1} \tag{19}$$

$$\bar{V}_{PN} = 0 \tag{20}$$

$$\bar{V}_{diode} = \bar{V}_{c1} + \bar{V}_{c2} \tag{21}$$

The average inductors voltage over one switching cycle at steady state is zero.

ISSN: 2233-7857 IJFGCN

3.4. Proposed SSE-RNN Controller

To make a controller plot the present work uses the combination of E-RNN and SSA for quasi-Z-source inverter. The E-RNN is a deep learning structure which is the combination of recurrent neural network (RNN). Jordasn and Elman are produced the most common RNNs where, Elman is partially RNN and Jordan is fully RNN. The outputs are generated without fluctuation and optimal outcomes are gotten quickly by using E-RNN. In the qZSI, the common mode voltage is higher than that in the conventional VSI because of shoot through state, which increases the higher leakage current and higher harmonics with decreases the inverter power efficiency. Thus, in the proposed framework utilize the SSA calculation for training the E-RNN to get the ideal output with harmonic reduction.

$$Objective\,function\,F(n) = \min(\mu_{qZSI}) \tag{22}$$

The objective function is calculated by () where, μ_{qZSI} is represented the THD of qZSI.

The structure of Elman-RNN is given in figure 2. Numerical depiction of Elman type RNN can be depicted as below. SSA depends upon the swarming behavior of salps and it acts as two groups i.e. leader and followers. The (V_{grid}) and (V_{diff}) are the grid voltage and difference voltage which are act as input to E-RNN and E-RNN output is (V_{crtl}). Here, $\tilde{A}, \tilde{B}, \tilde{C}, \tilde{D}$ are input, hidden, context and output layers and unit delay element is represented as z^{-1}. The Elman –RNN configuration to provide control voltage with harmonic is depicted in figure 5.

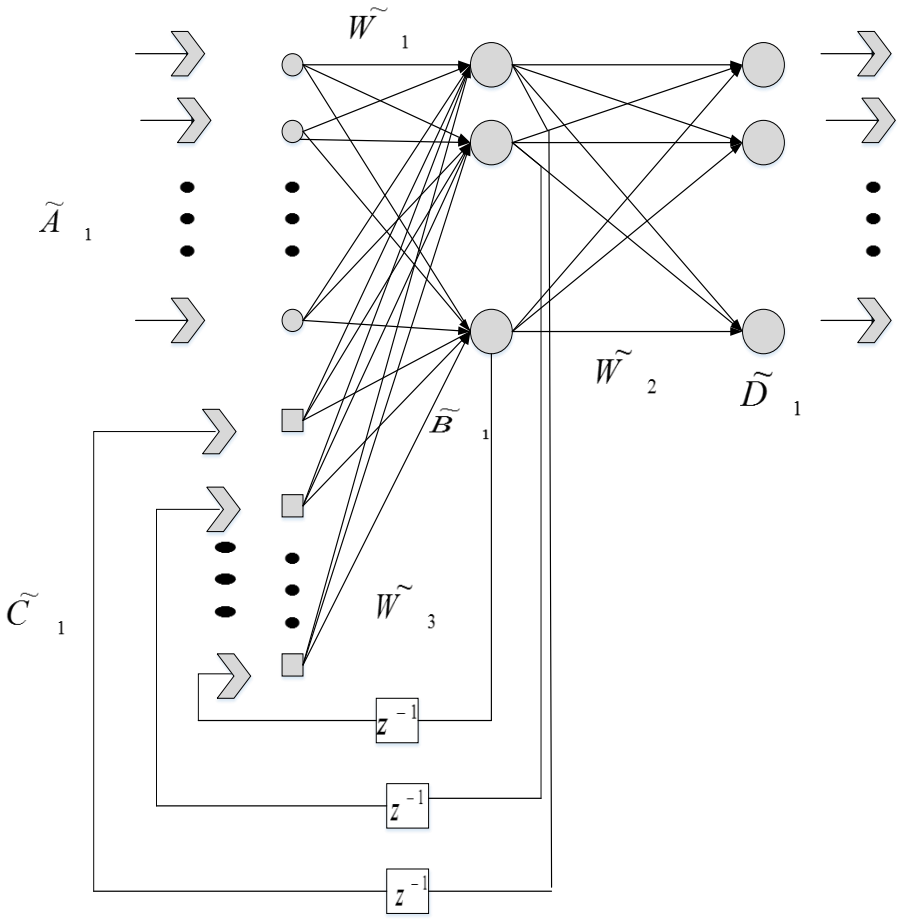

Figure 5. Structure of Elman-RNN

ISSN: 2233-7857 IJFGCN

3.4.1. Training of the Proposed Method: Elman-RNN is used to minimize the harmonics which are presented in the inverter. The weight and biases values of Elman-RNN are updated for the training process by SSA. In Elman, three weight matrix are considered as $\tilde{W}_1, \tilde{W}_2, \tilde{W}_3$, the weigh matrix between hidden and input layer is $\tilde{W}_1$, the weight matrix among the layer of output and hidden is $\tilde{W}_2$ and the weight matrix among the layer of hidden and context is $\tilde{W}_3$. All components of vector at nth iteration are given below:

$$a_i^{(n)} \in \tilde{A}_1 \,(\tilde{A}_1 = V_{grid} \,\&\, V_{diff}), \qquad i = 1,\ldots..,\, n \tag{23}$$

$$b_j^{(n)} \in \tilde{B}_1, \qquad j = 1,\ldots..,\, m \tag{24}$$

$$c_{i'}^{(n)} = \tilde{C}_1, \qquad i' = j \tag{25}$$

$$d_k^{(n)} \in \tilde{Z}_1 \,(\tilde{Z}_1 = V_{ctrl}), \qquad k = 1,\ldots..,\, l \tag{26}$$

Where, the number of input, hidden, context and output nodes are indicated by $i, j, i' \; and \; k$. And also, at nth iteration to compute the hidden node output for jth hidden node output consider the activation function $f(\cdot)$ which can be explained as follow,

$$b_j^{(n)} = f\left(a_j^{(n)}\right) \tag{27}$$

Where, at nth iteration the hidden node j at linear output is represented as $\left(a_j^{(n)}\right)$. At nth iteration the context layer input can also be expressed by,

$$c_{i'}^{(n)} = b_j^{s-1} \tag{28}$$

Elman neural network initial cases is expressed as follow,

$$b_j^{(0)} = 0, \; (j = 1,2,..m) \tag{29}$$

At n=1, the context layer input leads to $c_{i'}^{(1)} = 0$.

In terms of neural structure weight matrix, each and every coefficient of weight can be explained as a matrix element as,

$$w1_{ij} \in \tilde{W}_1, \quad w2_{jk} \in \tilde{W}_2, \quad w3_{ij} \in \tilde{W}_3 \tag{30}$$

Hence, for nth iteration the output of neuron in the output and hidden layer by weigh matrix can be calculated as follow

$$b_j^{(n)} = f\left(\sum_{i=1}^{n} w1_{ij}\, a_i^{(n)} + \sum_{j=1}^{m} w3_{ij}\, b_j^{(n-1)} \right), t = j \tag{31}$$

and

$$z_k^{(n)} = f\left(\sum_{j=1}^{m} w2_{jk}\, b_j^{(n)} \right) \tag{32}$$

And also, in the output layer the weight coefficient value is updated to minimized the MSE error E by

$$w^{new} = w^{old} + \Delta w \eta \tag{33}$$

ISSN: 2233-7857 IJFGCN

Where, learning rate is represented by η. For entire pattern vectors and nodes from output, E is explained with the below relationship.

$$E(w)=\frac{1}{2}\sum_{s=1}^{p}\sum_{k=1}^{l}\left[Z_k^n - z_k^n\right]^2 \tag{34}$$

Where, at nth iteration z_k^s is the target value.

Here, the length of training sequence is represented as p; $\tilde{W}_1$ and $\tilde{W}_3$ weight coefficient matrices can be familiar by the algorithm of back propagation, due to this network part which takes place among the layer of input and output which is in feed forward character.

Using the derivative chain rule for computation of $\tilde{W}_3$ which is described by,

$$\Delta w3_{ij} = -\frac{\partial E}{\partial b_j}\frac{\partial b_j}{\partial w3_{ij}} \tag{35}$$

Here, the first term is represented as follow,

$$\frac{\partial E}{\partial b_j^{(n)}} = \sum \frac{\partial E}{\partial z_k^{(n)}}\frac{\partial z_k^{(n)}}{\partial b_j^{(n)}} = -\sum_{k=1}^{l}\left[Z_k^n - Z_k^n\right] w2_{jk} \tag{36}$$

And the second term can be calculated as

$$\frac{\partial b_j^n}{\partial w3_{ij}^{(n)}} = f^1\left(b_j^n\right) b_j^{(s-1)} \tag{37}$$

Where, the derivation of activation function is indicated by $f'(\cdot)$. To compute the $\Delta w3_{tj}$ by last two derivations can be represented as,

$$\Delta w3_{ij} = \sum\left[Z_k^{(n)} - Z_k^{(n)}\right] w2_{jk}\, f'\left(b_j^{(n)}\right) b_j^{(n-1)} \tag{38}$$

Henceforth, this value is utilized to update the weight coefficient among hidden and context layer for training the technique of Elman-RNN. This work uses SSA to train the E-RNN operation to reach the objective function (22). Here, for training purpose we take certain amount of values to control the output voltage.

$$x_j^1 = V_{Ctrl} = \begin{cases} V_{grid} + c_1\left(\left(Ub_j - Lb_j\right)c_2 + Lb_j\right) & c_3 \geq 0 \\ V_{grid} - c_1\left(\left(Ub_j - Lb_j\right)c_2 + Lb_j\right) & c_3 \prec 0 \end{cases} \tag{39}$$

$$V_{grid} = \begin{cases} 0, if\ V > 350 \\ 1, if\ V < 450 \end{cases} \tag{40}$$

Where, upper bound and lower bound is represented as Ub_j & Lb_j, maximum iteration is represented as c_1, c_2, c_3, and grid voltage is denoted as V_{grid}. Thus, for training purpose we take 500 to 600 voltage and with this condition the other voltage can be automatically eliminated. In this iteration manner, the control voltage will be gotten very quickly. Thus, error free output voltage is generated by SSE-RNN and the overall performance is improved.

4. Results and Discussion

MATLAB/Simulink platform is utilized to implement the whole work. The performance such as current and voltage of inverter and current and voltage of grid, DC link performance and THD analysis. The performance of DC link and THD is compared with other existing controllers Ant Lion Optimizer-Neural Network (ALO-NN) [21] and fuzzy [22]. Figure 6 shows the proposed Simulink model.

ISSN: 2233-7857 IJFGCN

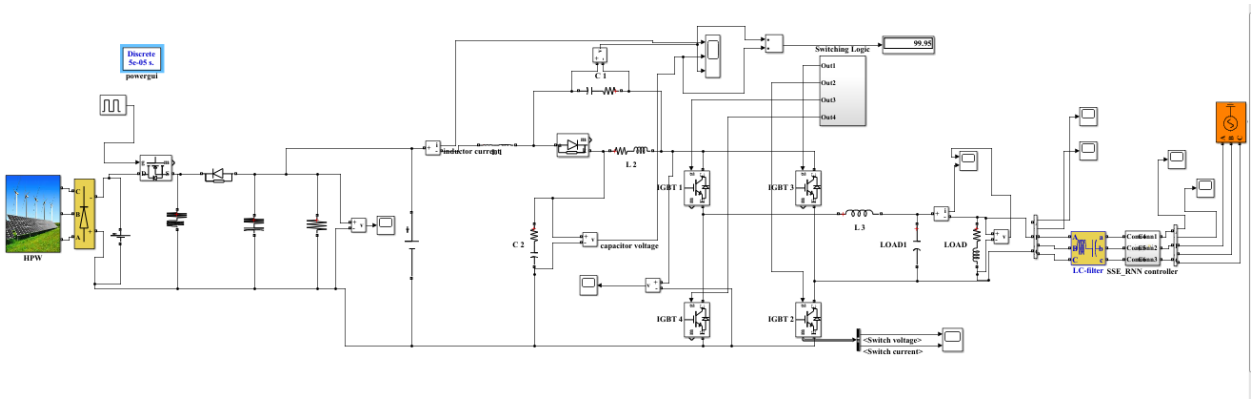

Figure 6. Proposed Simulink Model

The performance of inverter voltage is shown in figure 7. By varying time, the inverter voltage will be performed. Here, we got maximum amount of smooth voltage without harmonics by using our proposed SSE-RNN controller. To get the optimal inverter voltage without any harmonic distortion, the SSE-RNN controller is used for tuning purpose of inverter. Thus we get error free inverter voltage and not gotten the unbalanced output voltage.

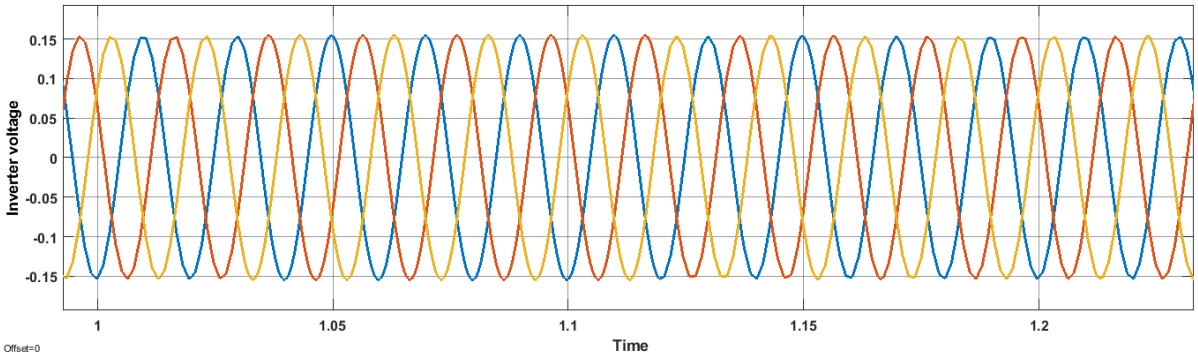

Figure 7. Inverter Voltage

The performance of inverter current is shown in figure 8. By varying time, the inverter current will be performed. Here, we got maximum amount of smooth inverter current without harmonics or any other distortion by using our proposed SSE-RNN controller. To get the optimal inverter current without unbalanced voltage and harmonic, the SSE-RNN controller is used for tuning the gate pulse inverter. Thus we get error free inverter current.

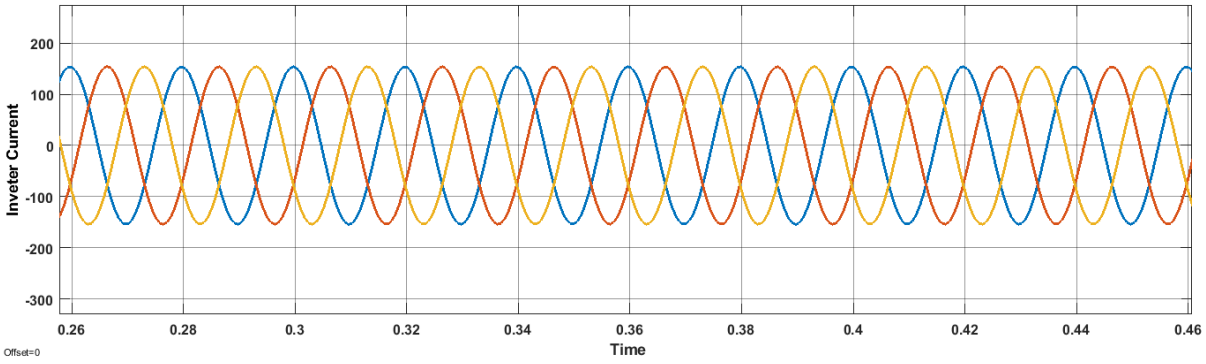

Figure 8. Inverter Current

The performance of grid voltage is shown in figure 9. By varying time, the grid voltage performance will be taken. Here, we got maximum amount of smooth inverter voltage without unbalanced voltage

ISSN: 2233-7857 IJFGCN

by using our proposed SSE-RNN controller. To get the optimal grid voltage without any harmonic distortion, the SSE-RNN controller is used for the tune the inverter. Thus we get error free inverter voltage.

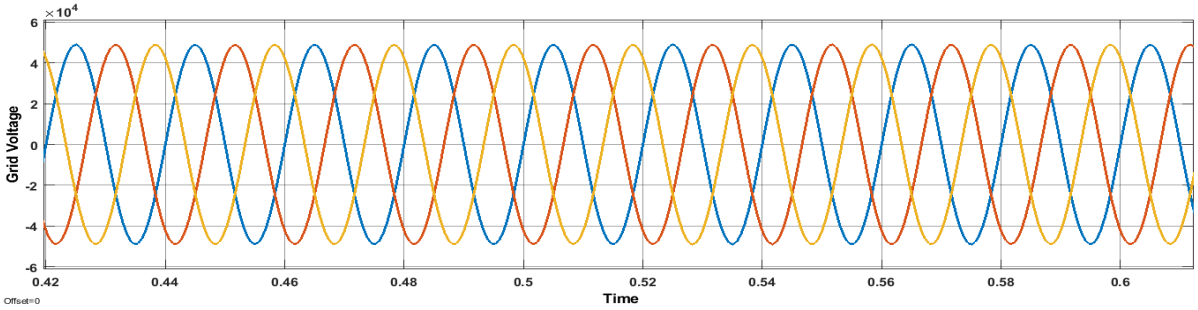

Figure 9. Grid Voltage

The performance of grid current is depicted in figure 10. The grid current will be performed based on time. Here, we got maximum amount of smooth grid current without harmonics by using our proposed SSE-RNN controller. This controller makes the output current as ideal and it generate the current without any harmonics. Thus we get error free grid current.

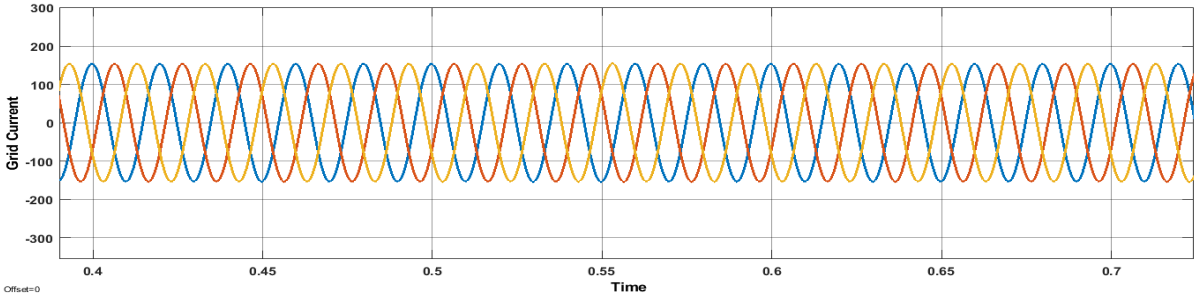

Figure 10. Grid Current

The performance of DC link volatge is shown in figure 11. Here, our proposed controller of SSE-RNN is compared with existing fuzzy and ALO-NN. The volatage value will be increased by varying time. The proposed SSE-RNN controller of DC link volatge is very high and the DC link voltage will stable very quickly than other existing algorithms.

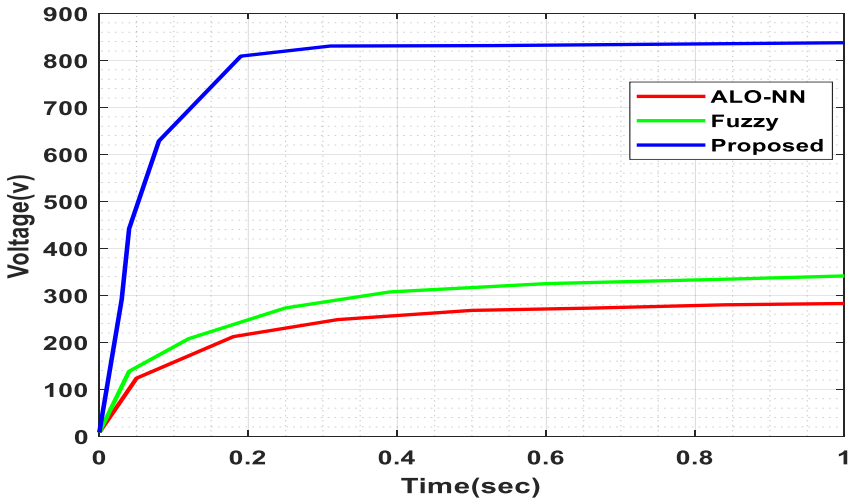

Figure 11. DC link Voltage

ISSN: 2233-7857 IJFGCN

Figure 12 shows the THD analysis at load side. By varying frequency, the magnitude value can be calculated and proposed THD is 0.17%.

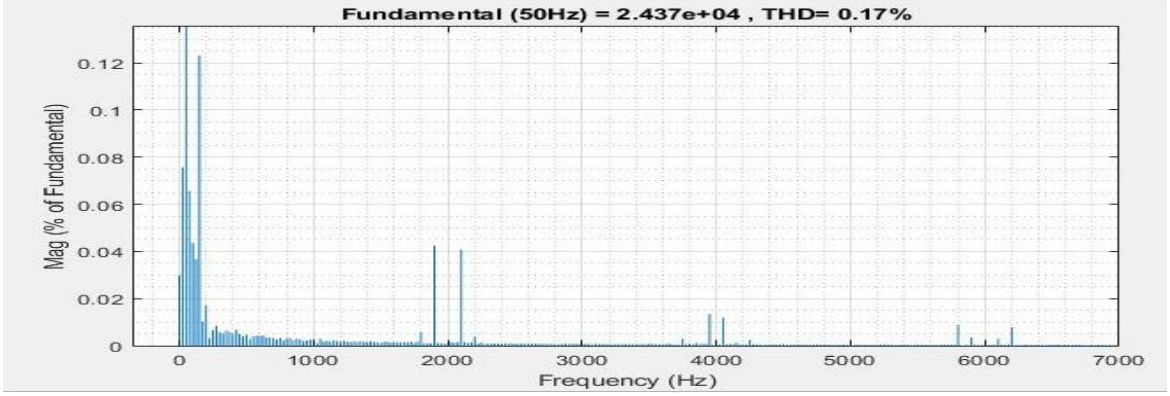

Figure 12. THD Analysis

The THD analysis of proposed method with existing techniques is given in table 1. THD analysis of existing fuzzy is 4.44%, existing ALO-NN is 0.8% and THD analysis of proposed method is 0.17%. comapred with existing values, our proposed method got better performance with low THD value. Thus, error free output voltage is generated by SSE-RNN and the overall performance is improved.

Table 1. THD Compariosn

S.No	Controller Used	THD%
1	Fuzzy	4.44
2	ALO-NN	0.8
3	Proposed	0.17%

5. Conclusion

This paper presented a qZSI with SSE-RNN controller for grid connected RES. Here, at inverter side, LC filter was used to improve the output due to the generation of less harmonic output voltages. Thus proposed SSE-RNN perform better in THD and reduced the design complexity. The performance outcome is inverter voltage and current, grid current, DC link voltage, grid voltage and the analysis of THD which is taken in MATLAB/Simulink Platform. The performance of THD and DC link voltage was compared with other existing techniques. In our method, we got 0.17% THD, thus our proposed method got better performance with low THD value. Thus, error free output voltage was generated by SSE-RNN and the overall performance was improved.

Reference

[1] H. Chu, X. Wang, X. Mou, M. Gao, H. Liu, "Cooperative Control Strategy of Hybrid Energy Storage System under Isolated Operation of Micro-grid", In Proceedings of PURPLE MOUNTAIN FORUM 2019-International Forum on Smart Grid Protection and Control, Springer, **(2020),** pp. 331-340.
[2] A. Aktaş, Y. Kırçiçek., "A novel optimal energy management strategy for offshore wind/marine current/battery/ultracapacitor hybrid renewable energy system", Energy, **(2020)**, p.117425.
[3] T. Wu, F. Ye, Y. Su, Y. Wang, S, Riffat, "Coordinated control strategy of DC microgrid with hybrid energy storage system to smooth power output fluctuation", International Journal of Low-Carbon Technologies, **(2020)**, vol. 15, no. 1, pp. 46-54.
[4] G. Varshney, D. S. Chauhan, M. P. Dave, "Grid connected solar PV system using carbon material based DYE sensitized solar cells", Materials Today: Proceedings, **(2020)**.

ISSN: 2233-7857 IJFGCN

[5] M.N. Ashtiani, A. Toopshekan, H. Yousefi and A. Maleki, "Techno-economic analysis of a grid-connected PV/battery system using the teaching-learning-based optimization algorithm", Solar Energy, **(2020)**, vol. 203, pp.69-82.
[6] Y. Ren, R. Duan, L. Chen, W. Huang, C. Wu and Y. Min, "Stability Assessment of Grid-connected Converter System Based on Impedance Model and Gershgorin Theorem", IEEE Transactions on Energy Conversion, **(2020).**
[7] H. Chen, Z. Zhang, C. Guan and H. Gao, "Optimization of sizing and frequency control in battery/supercapacitor hybrid energy storage system for fuel cell ship", Energy, **(2020)** p.117285.
[8] D. Shunmugham Vanaja and A.A. Stonier, " A novel PV fed asymmetric multilevel inverter with reduced THD for a grid-connected system", International Transactions on Electrical Energy Systems, **(2020)** p.e12267.
[9] W. Jiang, K. Ren, S. Xue, C. Yang and Z. Xu, "Research on The Asymmetrical Multilevel Hybrid Energy Storage System Based on Hybrid Carrier Modulation", IEEE Transactions on Industrial Electronics, **(2020)**
[10] M.H. Prabhu and K. Sundararaju, "Power quality improvement of solar power plants in grid connected system using novel Resilient Direct Unbalanced Control (RDUC) technique", Microprocessors and Microsystems, **(2020)**, vol. 75, p.103016.
[11] N. Singh and S.K. Jain, "Investigation of three-level NPC-qZS inverter-based grid-connected renewable energy system", IET Power Electronics, **(2020)**, vol. 13, no. 5, pp.1071-1085.
[12] Ł. Bartela, "A hybrid energy storage system using compressed air and hydrogen as the energy carrier", Energy, **(2020),** vol. 196, p.117088.
[13] R. Sood and G. Kalpesh, "THD reduction and power quality improvement in grid connected PV system", **(2020)**.
[14] A. Amir, A. Amir, J. Selvaraj and N. Abd Rahim, "Grid-connected photovoltaic system employing a single-phase T-type cascaded H-bridge inverter", Solar Energy, **(2020),** vol. 199, pp.645-656.
[15] H. Chen, D. Xu and X. Deng, "Control for Power Converter of Small-scale Switched Reluctance Wind Power Generator", IEEE Transactions on Industrial Electronics, **(2020).**
[16] M. Jafari and Z. Malekjamshidi, "Optimal energy management of a residential-based hybrid renewable energy system using rule-based real-time control and 2D dynamic programming optimization method", Renewable Energy, **(2020)**, vol. 146, pp.254-266.
[17] D. Rekioua, " Storage in Hybrid Renewable Energy Systems", In Hybrid Renewable Energy Systems, Springer, **(2020)**, pp. 139-172.
[18] A. Chakir, M. Tabaa, F. Moutaouakkil, H. Medromi, M. Julien-Salame, A. Dandache and K. Alami, "Optimal energy management for a grid connected PV-battery system", Energy Reports, **(2020)**, vol. 6, pp.218-231.
[19] T. Guo, Y. Liu, J. Zhao, Y. Zhu and, J. Liu, "A dynamic wavelet-based robust wind power smoothing approach using hybrid energy storage system", International Journal of Electrical Power & Energy Systems, **(2020)**, vol. 116, p.105579.
[20] D. Rekioua, "MPPT Methods in Hybrid Renewable Energy Systems", In Hybrid Renewable Energy Systems, Springer, **(2020)**, pp. 79-138.
[21] J. Phalke, H.H. Kulkarni and A.P. Student, "Grid Tied Solar Inverter at Distribution Level with Power Quality Improvement", Journal of Emerging Technologies and Innovative Research, **(2014)**, vol. 1, no. 3.
[22] M.D. Patil and K. Vadirajacharya, "ALO optimized Neural Network Controlled Three Phase Five Level Cascaded H-Bridge Inverter for Integrating PV Panel with Smart Grid", Jour of Adv Research in Dynamical & Control Systems, **(2018)**, vol. 10, no. 9.

ISSN: 2233-7857 IJFGCN